Available online at www.sciencedirect.com
ScienceDirect
Journal of Nutritional Biochemistry 21 (2010) 818–826
Journal of Nutritional Biochemistry

# 4-Hydroxynonenal, a lipid peroxidation product of dietary polyunsaturated fatty acids, has anticarcinogenic properties in colon carcinoma cell lines through the inhibition of telomerase activity☆

Stefania Pizzimenti[a,*,1], Elisa Menegatti[b,1], Daniela Berardi[b], Cristina Toaldo[a], Piergiorgio Pettazzoni[a], Rosalba Minelli[a], Barbara Giglioni[c], Angelo Cerbone[a], Mario U. Dianzani[a], Carlo Ferretti[d], Giuseppina Barrera[a]

[a]Department of Medicine and Experimental Oncology, Section of General Pathology, University of Turin, 10125 Torino, Italy
[b]Department of Experimental Medicine and Oncology, Section of Clinical Pathology, University of Turin, 10125 Torino, Italy
[c]Institute of Molecular Bioimaging and Physiology (IBFM), National Research Council (CNR), 20090 Segrate (Milano), Italy
[d]Department of Anatomy, Pharmacology and Forensic Medicine, University of Turin, 10125 Torino, Italy.

Received 20 March 2009; received in revised form 8 June 2009; accepted 15 June 2009

**Abstract**

The effects of polyunsaturated fatty acids (PUFAs) obtained from the diet on colorectal cancer have been widely explored. However, controversial results have been obtained about the role played by the lipid peroxidation products of PUFAs, such as 4-hydroxy-nonenal (HNE), in the control of colon cancer growth. This aldehyde, indeed, showed both procarcinogenic and protective effects. In an attempt to verify the action of HNE, we studied the effects of a low dose of HNE (1 μM), similar to those "physiologically" found in normal cells and plasma, on telomerase activity, a key parameter of malignant transformation. Caco-2 cells were exposed to HNE and, paralleling cell growth inhibition, we observed the down-regulation of telomerase activity and *hTERT* expression. Similar effects have also been observed in HT-29 cells, in which HNE inhibited cell proliferation, telomerase activity and *hTERT* expression, suggesting that the inhibition of telomerase activity could be a general mechanism involved in the antiproliferative effect exerted by this aldehyde. Finally, we elucidated the mechanism of *hTERT* inhibition by HNE. A reduction of GSH content preceded the decrease of telomerase activity, but this only partially explained the telomerase activity inhibition. The major mechanism of HNE action seems to be the modulation of expression and activity of transcription factors belonging to the Myc/Mad/Max network.

Since the presence of PUFAs in the diet exposes epithelial colon cells to HNE, this aldehyde could contribute to cell growth control through the inhibitory action on telomerase activity and *hTERT* expression, suggesting a protective effect on colon mucosa.


*Keywords:* 4-Hydroxynonenal; Caco-2; HT-29; Telomerase activity; *hTERT* gene expression, GSH; Myc/Mad/Max network

## 1. Introduction

Polyunsaturated fatty acids (PUFAs) cannot be synthesized in mammals and they must be obtained from the diet. Their effects in colorectal cancer have been widely explored [1,2]. However, controversial results have been obtained about the role played by the lipid peroxidation products of PUFAs in the control of colon cancer growth. The induction of lipid peroxidation largely results from free radical reactions. The unsaturated bonds of PUFAs undergo the auto catalytic process of peroxidation which produces a complex mixture of end-products, including a series of 4-hydroxy-alkenals. Among them, 4-hydroxy-2-nonenal (HNE) is the most intensively studied [3]. Intriguingly, free radical species and HNE can have both carcinogenic and pro-apoptotic effects.

Several authors demonstrated that HNE has mutagenic and genotoxic effects on prokaryotic systems or eukaryotic cell lines, mainly through the formation of HNE-DNA adducts [4]. Hu et al. [5] demonstrated that the formation of HNE-dG adducts may contribute greatly to G→A transition at codon 249 of the p53 gene, and this may play an important role in carcinogenesis. However, HNE has been demonstrated to have pro-apoptotic effects on several cell lines, through the involvement of numerous pathways, such as c-Jun N-terminal kinase, p38 mitogen-activated protein kinase, tyrosine kinase receptors, Akt/PKB protein kinase [6], the death receptor Fas

☆ Supported by grants from *Compagnia di San Paolo* and University of Turin (ex 60%) funds (G.B.).
* Corresponding author. Dipartimento di Medicina ed Oncologia Sperimentale, Sezione di Patologia Generale, 10153 Torino, Italy. Tel.: +39 011 6707763; fax: +39 011 6707753.
*E-mail address:* stefania.pizzimenti@unito.it (S. Pizzimenti).
[1] S.P. and E.M. have contributed equally to the studies present in this manuscript.

0955-2863/$ – see front matter © 2010 Elsevier Inc. All rights reserved.
doi:10.1016/j.jnutbio.2009.06.005

(CD95)-mediated extrinsic pathway and the p53-dependent intrinsic pathway [7]. Moreover, HNE is able to induce differentiation in several leukemia cell lines [8–10] and exerts its antiproliferative effect by modulating the expression of several genes involved in the control of the cell cycle, such as oncogenes [9,11,12], cyclins and their inhibitor p21 [13,14], transcription factors [14,15] and tumor suppressors [16]. Recently, this double-edged sword property has been outlined in different reviews [17–19].

In an attempt to study the role of oxidative stress in cell growth control, several research groups have considered the biological effects of HNE because this aldehyde is more stable than free radicals, it can diffuse from the site where it is produced and it can reach different intracellular and extracellular targets [3,7,20]. Recently, we demonstrated that HNE induced cellular senescence in leukemic cell lines by inhibiting telomerase activity and the expression of the *hTERT* gene, the catalytic subunit of telomerase [21]. Reactivation of telomerase activity, the enzyme essential for the maintenance of replicative potential in cells, is a crucial event in tumorigenesis. Telomerase is expressed in embryonic cells, but it is not expressed in most somatic cells, with the exception of regenerative tissues, such as germline cells, hematopoietic stem cells and lymphocytes [22]. In tumors, reactivation of telomerase activity represents an important step, leading tumor cells to escape from senescence [23,24]. Telomerase activity decreases during terminal differentiation of human and murine immortalized cells in response to pharmacological agents [25–27]. In colon cancer, as expected, telomerase activity and *hTERT* gene expression are significantly higher with respect to normal colon mucosa [28,29]. Moreover, a progressive increase of *hTERT* expression and telomerase activity from adenomas to invasive colon carcinoma has been demonstrated in patients [30,31].

Colon epithelial cells can be physiologically exposed not only to fatty acids but also to lipid peroxidation end products, such as HNE, originated by dietary PUFAs [32], as also demonstrated by the presence of HNE in faecal water [33].

For this reason, we investigated the effects of HNE on cell proliferation, differentiation, apoptosis and telomerase activity in colon cancer cells. Human colon carcinoma Caco-2 cells were exposed to a low dose of HNE (1 μM), similar to those "physiologically" found in normal cells and plasma [34]. Moreover, in order to determine whether HNE produced similar effects in other colon cancer cell lines, telomerase activity and *hTERT* expression were also studied in human colon cancer HT-29 cells. In an attempt to investigate the HNE mechanisms in inhibiting telomerase activity, the content of reduced glutathione (GSH), the natural scavenger of HNE [34], was analyzed since reduced GSH content has been found to parallel decreased telomerase activity [35]. Moreover, since the major control mechanism of telomerase activity seems to be the regulation of *hTERT* expression, which, in turn, is regulated by three major transcription factors (Myc, Mad-1 and Sp-1) [36,37], we investigated in HNE-treated cells, the regulation of *hTERT* promoter activity.

## 2. Materials and methods

### 2.1. Cells and culture conditions

Caco-2 and HT-29 colon carcinoma cells, obtained from European Collection of Cell Cultures, were cultured at 37°C in a humidified atmosphere of 5% $CO_2$ air. For all experiments, cells from 1 to 10 passages were used. Caco-2 cells were grown in Dulbecco's modified eagle medium (D-MEM) medium supplemented with 2 mM glutamine, 10% foetal calf serum (FCS) (Biochrom Seromed, Berlin, Germany), 1% nonessential amino acids solution and 1% antibiotic mixture (penicillin-streptomycin) (Sigma, Milano, Italy). HT-29 cells were grown in RPMI 1640 medium supplemented with 2 mM glutamine, 1% antibiotics and 10% FCS (Biochrom Seromed).

### 2.2. Cell treatments

Repeated treatments with HNE were performed by adding 1 μM HNE (Calbiochem, La Jolla, CA, USA) to the cells at regular intervals of time (45 min) up to 10 treatments (the overall time of exposure to the aldehyde was 7.5 h) as previously described [8]. This experimental procedure was used because 1 μM HNE disappears from the culture medium within 45 min and must be repeatedly added to activate the differentiation program in HL-60 cells [8].

Caco-2 cells treated with 2 and 10 mM butyrate (Sigma) were used as positive control for differentiation and apoptosis, respectively.

### 2.3. Assay of cell growth and cell viability

Caco-2 were seeded, about 4000 cells per well, in a 96-well plate and cell proliferation was evaluated by using the kit "CellTiter96-Non Radioactive Cell proliferation Assay" (Promega, Milano, Italy). This highly sensitive assay detects the luminescence released by the metabolically active cells. Quantification of luminescence was expressed as relative light unit (RLU) (Luminescence Spectometer LS 55; Perkin Elmer, Milano, Italy). Cytotoxicity was measured by the kit "CellTiter-Glo Luminescent Cell Viability Assay" (Promega), according to the manufacturer's protocol. This reaction develops colour detected by measuring the absorbance at 570 nm by an enzyme-linked immunosorbent assay (ELISA) plate reader (Bio-Rad Laboratories, Segrate, Italy).

HT-29 cell growth was determined by the 3-(4,5-dimethylthiazol-2-yl)-2,5-diphenyltetrazolium bromide (MTT) assay, which is based on the conversion of the yellow tetrazolium dye MTT to purple formazan crystals by metabolically active cells. HT-29 cells were seeded, 4000 cells per well, in a 96-well plate. After HNE treatment, 30 μl MTT dye solution [5 mg/ml in phosphate-buffered saline (PBS) 1×] were added to each well, and the plate was incubated for 3 h at 37°C. Dimethyl sulphoxide (150 μl) was added for 20 min and the absorbance at 540 nm was recorded using an ELISA plate reader (Bio-Rad Laboratories).

### 2.4. Detection of apoptotic cells

Apoptosis in Caco-2 HNE-treated cells was detected by the terminal deoxynucleotidyl transferase dUTP nick end-labeling (TUNEL) method. The TUNEL method from Promega consists of the terminal deoxynucleotydil transferase-mediated nick-end labelling of fluorescein isothiocyanate FITC-conjugated deoxyuridine triphosphate. Briefly, cells cultured in the four-well chambers (800,000/ml) were treated with HNE and, at the indicated times, fixed in 4% paraformaldehyde for 30 min and washed for 5 min. The manufacturer's protocol was then followed. Incorporated fluorescein was detected using a fluorescence microscope (Leitz, Dialux 20, Oberkochen, Germany). The number of apoptotic cells was determined by counting the percentage of green fluorescence-positive cells. At least 100 cells were counted for each experiment (three separate experiments from three different preparations for each condition).

Caco-2 cells treated with 10 mM butyrate were used as positive control of apoptosis.

### 2.5. Detection of differentiated cells

Caco-2 cell differentiation was determined by counting the dome formation in control or HNE-treated cells. Dome formation, which can be attributed to ion and water transport across polarized epithelial cells [38], was quantified in confluent CaCo-2 monolayers using inverted light microscopy and expressed as the number of domes per square centimetre. Domes were recognised as a cohesive group of approximately 30 cells or more that were in a different plane of view compared to cells attached to the culture plate.

Caco-2 cells treated with 2 mM butyrate were used as positive control of differentiation.

### 2.6. RNA isolation and semiquantitative reverse transcriptase–polymerase chain reaction analysis

RNA analyses were performed by a semiquantitative polymerase chain reaction (PCR) method as previously described [13]. Briefly, the experimental strategy included the following precautions: (1) the number of PCR cycles was kept low in order to obtain an exponential amplification of PCR products; (2) all results were standardised using the signal obtained with glyceraldehyde 3-phosphate dehydrogenase (GAPDH); (3) all experiments were performed with at least three independent cDNA preparations; (4) to control for DNA contamination, primers were designed to span at least one exon-intron boundary. Total RNA was isolated using the RNA fast Kit (Molecular System, Genenco, Milano, Italy). cDNA synthesis was performed with 4 μg of total RNA in a reaction volume of 40 μl containing 1.25 μg of random primers; 1 mM of dATP, dGTP, dCTP and dTTP (Invitrogen, Milano, Italy); 66 U of RNAguard (Amersham Biosciences, Cologno Monzese, Milano, Italy); 8 μl of 5× first-strand buffer; 10 mM DTT and 300 U of MMLV reverse transcriptase (Invitrogen). Samples were incubated for 1 h at 37°C and the reaction was stopped by heating for 10 min at 95°C. PCR reactions were performed in a GeneAmp PCR System 9600 (Perkin Elmer), with 1 μl of cDNA reaction mixture in a volume of 50 μl containing 200 μM of dATP, dTTP, dGTP and dCTP; 1 μM of 5′- and 3′-primer and 1.25 U of TAQ DNA polymerase (Finnzymes, Milano, Italy). Samples were subjected to denaturation at 95°C for 45 s, annealing (30 s at 58°C for *hTERT* primers, 1 min at 60°C for c-*myc* and mad-1 primers, 30 s at 64°C for sp-1 primers, 1 min at 52°C for GAPDH primers) and extension at 72°C for 45 s, followed by a final extension at 72°C for 3 min. Negative controls contained water instead of cDNA. The primer pair

sequences used for PCR amplification and the numbers of PCR cycles done are indicated as follows:

*hTERT*: 33 cycles
(forward primer): 5′-ACGGCGACATGGAGAACAA-3′
(reverse primer): 5′-CACTGTCAACCGCAAGTTCAC-3′
amplifying a 175-bp fragment.
c-*myc*: 35 cycles
(forward primer): 5′- GAGACAACGACGGCGGTG -3′
(reverse primer): 5′-GCTCGTTCCTCCTCTGGC -3′
amplifying a 788-bp fragment.
mad-1: 35 cycles
(forward primer): 5′- CCAGGTGGAGCGGGAGAAAATGC-3′
(reverse primer): 5′- CCACTGCAGTTCCGAGATCCTCC-3′
amplifying a 318-bp fragment.
sp-1: 33 cycles
(forward primer): 5′- ACAGGTGAGCTTGACCTCAC-3′
(reverse primer): 5′- GTTGGTTTGCACCTGGTATG-3′
amplifying a 369-bp fragment.
GAPDH: 25 cycles
(forward primer): 5′-GTCGGAGTCAACGGATTTGG-3′
(reverse primer): 5′-GGGTGGAATCATATTGGAACATG-3′
amplifying a 119-bp fragment.

A 10-μl sample of the PCR reaction mixture was separated on a 1% agarose gel and amplification products were stained with GelStar nucleic acid gel staining (FMC BioProducts, Rockland, ME, USA). Densitometric analysis was performed by using a software program (Multi-Analyst, version 1.1, Bio-Rad Laboratories).

### 2.7. Telomerase activity

#### 2.7.1. Samples collection and extraction

Telomerase was extracted from the Caco-2 and HT-29 cells; $5\times10^6$ cells were seeded and resuspended in 200 μl of 3-[(3-cholamidopropyl)dimethylammonio]-1-propanesulfonate (CHAPS) lysis buffer, containing 0.5% CHAPS, 1 mM $MgCl_2$, 10% glycerol, 10 mM Tris HCl pH 7.5, 1 mM ethylene glycol-bis(2-aminoethylether)-*N*,*N*,*N*′,*N*′-tetraacetic acid, di 0.1 mM phenylmethylsulphonyl fluoride (PMSF) and 5 mM β-mercaptoethanol (Sigma-Aldrich). After 30 min of incubation on ice, the lysates were centrifuged at 16,000×*g* for 20 min at 4°C, and the supernatant was rapidly frozen and stored at −80°C.

#### 2.7.2. Telomerase assay

Telomerase activity was assayed by a modification of conventional TRAP assay [24], as described by Gelmini et al. [39]. This method is based on the use of a sensitive fluorochrome that selectively binds double-stranded DNA. Because telomerase, contained in a protein extract, generates double-stranded DNA by adding nucleotide to a primer and because the amount of newly synthesized DNA is proportional to telomerase activity, the measurement of DNA concentration in post-PCR samples can be considered quantitatively related to telomerase activity [39]. Each sample was assayed for telomerase activity in duplicate, starting from protein extracts of cell lines. A negative control, obtained after pre-treatment of the sample with RNase, was also assayed for each specimen. The protein concentration was measured in each extract by the Bio-Rad Protein Assay (Bio-Rad Laboratories). An aliquot of extract containing 3 μg of protein was used for each duplicate. RNase (Roche Diagnostic, Monza, Milano, Italy) was used at 0.5 μg/assay for 30 min at 37°C to inactivate telomerase. Each extract was assayed in 47.2 μl of reaction mixture containing 10 mM Tris–HCl pH 8.3, 50 mM KCl, 4.5 mM $MgCl_2$, 1 mM each dNTP, 20 pmol of TAG-U primer [39] and 0.5 μM $T_4$ gene 32 protein (Roche Diagnostic). After 60 min incubation at 30°C for telomerase-mediated extension of TAG-U primer, the reaction mixture was heated at 90°C for 3 min and then subjected to 50–60 PCR cycles of 95°C for 30 s, 64°C for 30 s and 72°C for 30 s, followed by 72°C for 10 min after the addition of 2.8 μl of a second reaction mixture containing 20 pmol of CTA-R primer [39] and 0.3 μl of 5 U/μl of Taq Gold (Applera Italia, Monza, Italy). Ten microliters of each PCR product was diluted with 490 μl of 10 mM Tris–HCl, 1 mM EDTA pH 7.5 (Sigma-Aldrich) and then 500 μl of ultrasensitive fluorescent dye PicoGreen (Molecular Probes, Leiden, The Netherlands; 1:1000 diluted stock solution) was added. Fluorescence was measured in a Luminescence Spectrometer LS 55 (Perkin Elmer) using standard wavelengths (excitation at 480 nm, emission at 520 nm). The DNA concentration was calculated for each sample on a calibration curve generated by dilutions of a control DNA (0–100 μg/L). The final DNA concentration of each sample was obtained by subtracting the DNA amount obtained in the same specimen after RNase treatment. Telomerase activity was calculated as the mean of duplicates, expressed in terms of nanograms of DNA per microgram of protein and reported in figures as percentage of control sample.

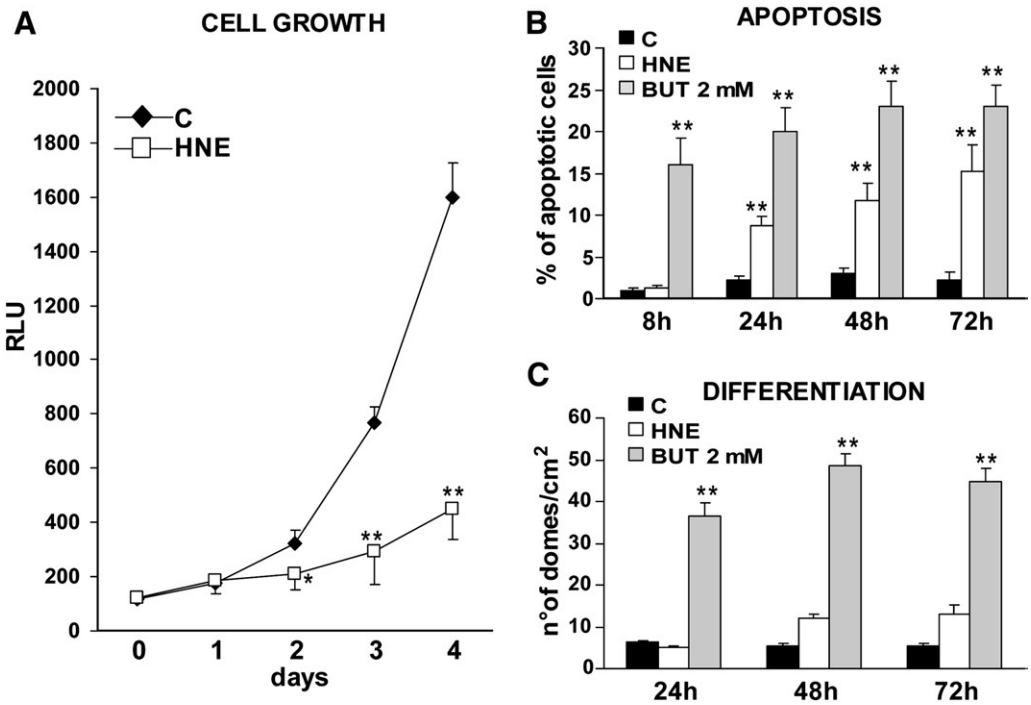


Fig. 1. Cell proliferation, apoptosis and differentiation in HNE-treated Caco-2 cells. (A) Caco-2 cell proliferation in untreated (C) and HNE -treated cells (10 repeated treatments with 1 μM HNE). Cell proliferation was detected by measuring the luminescence released by the metabolically active cells. The values, expressed in RLU are the means±S.D. of four separate experiments. Variance analysis: *$P$<.05; **$P$<.01 vs. control. (B) Apoptosis in Caco-2-untreated cells (C), HNE-treated cells (10 repeated treatments with 1 μM HNE); 10 mM butyrate (BUT 10 mM) was used as positive control. Apoptosis was detected by TUNEL test at the indicated time. Results are expressed as percentage of fluorescent cells and are the means±S.D. of three separate experiments from three different preparations or each condition. Variance analysis: **$P$<.01 vs. control. (C) Caco-2 differentiation in untreated (C) and HNE -treated cells (10 repeated treatments with 1 μM HNE); 2 mM butyrate (BUT 2 mM) was used as positive control. Differentiation was detected by counting the dome formation at the indicated time and expressed as numbers of domes per $cm^2$. The values are the means±S.D. of three separate experiments three and different preparations of each condition. Variance analysis: **$P$<.01 vs. control.

### 2.8. GSH content

For determination of GSH content, $4\times10^6$ Caco-2 cells were seeded in culture flasks, collected at 8, 24 and 48 h from the beginning of HNE treatment, in PBS 1× with a cell scraper. After centrifugation, cells were resuspended in a lysis buffer containing Hepes pH 7.9 10 mM, MgCl2 1.5 mM, KCl 10 mM, 1% Triton, 1 mM sodium orthovanadate, 1 mM PMSF and 0.05% aprotinin for cytosolic protein extraction. Samples were centrifuged at 1900 RPM for 10 min at 4°, and the supernatant was collected and centrifuged at 10,000×*g* for 20 min at 4°C. The supernatant was collected and the protein content was measured by using the commercially available Bio-Rad protein assay (Bio-Rad Laboratories).

GSH content was determined by the Owens and Belcher procedure [40]. Briefly, the cytosolic protein fraction (100 μl) was mixed with 0.05 M Na-phosphate buffer, pH 7.0, 1 mM EDTA pH 7.0 and 10 mM 5,5′-dithiobis-2-nitrobenzoic acid in cuvette. The mixture was incubated for 1 min at room temperature and the absorbance was monitored at 412 nm for 2 min using a spectrophotometer. The concentration of GSH in the cell lysate was calculated using a standard curve and expressed as μmoles of GSH per mg of protein. GSH content was then expressed as percentage of control.

### 2.9. Preparation of nuclear extracts

Caco-2 nuclear protein extracts were obtained from control and HNE-treated cells, by using the Nuclear Extract Kit (Active Motif, Carlsbad, CA, USA), according to the manufacturer's protocol.

### 2.10. DNA binding activity of c-Myc, Mad-1 and Sp-1 transcription factors

The c-Myc, Mad-1 and Sp-1 DNA binding activity assays in Caco-2 cell extracts were performed by using Trans-AM ELISA-based kits from Active Motif according to the manufacturer's protocol. Briefly, 2.5 μg of nuclear extracts from control and HNE-treated cells were incubated in a 96-well plate coated with an oligonucleotide containing the E-box motif (5′-CACGTG-3′) or the GC-box motif (5′-GGGCGG-3′). Activated transcription factors from extracts, specifically bound to the respective immobilized oligonucleotide, were detected using the antibody to c-Myc, Mad-1 or Sp-1. Activated transcription factors from extracts, specifically bound to the respective immobilized oligonucleotide, were detected using the antibody to c-Myc, Mad-1 or Sp-1 followed by a secondary antibody conjugated to horseradish peroxidase in an ELISA-like assay. The absorbance at 450 nm was recorded by an ELISA plate reader (Bio-Rad Laboratories).

### 2.11. Generation of hTERT-GFP constructs

After cloning of the *hTERT* promoter in 1999 [41], deletion analysis identified the proximal 200–300-bp region functioning as the core promoter, essential for cancer-specific transcriptional activation [42]. Two constructs containing the core promoter of *hTERT* (sequence available on NCBI Gene Bank, accession number AF098956) were generated by PCR, by using as template DNA from healthy blood donor leukocytes. The first fragment (284 bp) spans a region between −279 and +5 of *hTERT* promoter; it contains one E-box and five GC-boxes, and it corresponds to the *hTERT* minimal core promoter [41]. The second one (154 bp) spans a region between −149 and +5 of *hTERT* promoter and it corresponds to the E-box deleted form of the minimal core promoter.

The primers used for amplification of the 284- and 154-bp fragments were, respectively: 5′-gatacgagatctgacccccgggtccg-3′ (forward) and 5′-gatacggaattcgctgcct-gaaactcgcgcc-3′ (reverse); 5-gatacgagatctgccccttcaccttccagc-3′ (forward) and 5′ gatacggaattcgctgcctgaaactcgcgcc-3′(reverse). PCR products sequence was checked by direct sequencing (3100 Avant Genetic Analyzer, Applied Biosystems, Milano, Italy).

After digestion with *Eco*RI and *Bam*HI, the two fragments were cloned into the multicloning site of pmaxFP-Green-PRL (Amaxa, Cologne, Germany) upstream of the maxFP-Green coding sequence, an improved variant of maxGFP cloned from copepod (*Pontellina plumata*) [43]. Orientation and sequence of each insert were checked by automatic sequence analysis (3100 Avant Genetic Analyzer, Applied Biosystems). The constructs were named Ebox-*hTERT*-GFP (containing the 284 bp fragment) and Ebox-less-*hTERT*-GFP (containing the 154 bp fragment).

The plasmids were propagated in *Escherichia coli* Competent Cells (Promega) employing standard procedures and purified employing the EndoFree Plasmid Maxi Kit (QIAGEN, Milano, Italy).

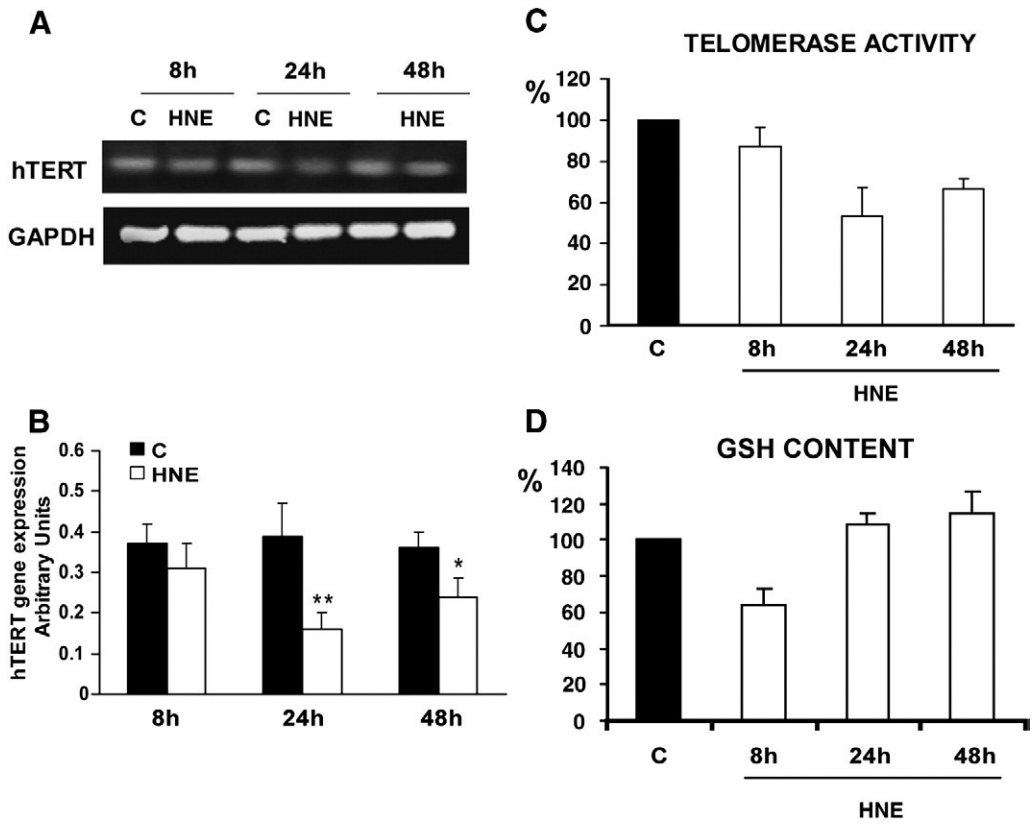


Fig. 2. *hTERT* expression and telomerase activity in HNE-treated Caco-2 cells. (A) *hTERT* mRNA levels determined by RT-PCR in Caco-2-untreated cells (C) and in HNE-treated cells (10 repeated treatments with 1 μM HNE) at the indicated time. (B) the relative quantification of RT-PCR products performed by densitometric scanning is shown. Data were normalized using the GAPDH signal and expressed as arbitrary densitometric units. Values represent the means±S.D. of three independent experiments. Variance analysis: *$P\leq.05$; **$P\leq.01$ vs. control. (C) Telomerase activity. The activity was evaluated at the indicated times in Caco-2-untreated cells (C) and in HNE-treated cells (10 repeated treatments with 1 μM HNE) at the indicated time. Telomerase activity was calculated in terms of nanograms of DNA produced per microgram of protein from three independent experiments and reported in figures as percentage of control sample. (D) GSH content. The GSH content was evaluated in Caco-2-untreated cells (C) and in HNE-treated cells (10 repeated treatments with 1 μM HNE) at the indicated time. GSH content was calculated in terms of nanomoles of GSH per milligram of protein from three independent experiments and reported in figures as percentage of control sample. RT-PCR, reverse transcriptase–PCR.

*2.12. Transient transfection*

For transfection experiments, Caco-2 cells were seeded into six wells and grown until 80% confluence; 4 μg of Ebox-*hTERT*-GFP or Ebox-less-*hTERT*-GFP plasmid constructs were transfected using Lipofectamine 2000 reagent (Invitrogen, Milano, Italy), according to the manufacturer's instruction. Four hours after transfection, cells were treated with HNE and promoter activity was determined at 24 h by analyzing maxFP-Green expression by Western blot.

Cells transfected with the promoter-less pmaxFP-Green-PRL vector were used as negative control. For positive control, pmaxGFP plasmid (Amaxa) encoding the maxGFP protein, under the control of the cytomegalovirus promoter pCMV, was used. At least three independent experiments for each condition were performed.

*2.13. Preparation of total extracts and Western blot analysis*

$5\times10^6$ Caco-2 cells were washed twice in cold PBS, pH 7.4. Total extracts were prepared by lysis in a buffer containing Tris-HCl buffer, pH 7.4, 150 mM NaCl, 5 mM EDTA, 1% Nonidet P-40, 1 mM sodium orthovanadate, 1 mM PMSF and 0.05% aprotinin. After high-speed centrifugation at 4°C, supernatant was collected and the protein concentration was measured in triplicate using the commercially available Bio-Rad protein assay (Bio-Rad Laboratories).

Five micrograms of proteins were separated by electrophoresis in 9.3% polyacrilamide gel (Bio-Rad Mini Protean II system). Proteins were electroblotted to nitrocellulose membranes (GE Healthcare, Milano, Italy) using the Biometra-Fast-Blot, a semidry blotting apparatus (400 mA, 30 min) (Biometra, Goettingen, Germany). Membranes were blocked overnight at 4°C in Tris-buffered saline containing 5% milk plus 0.5% Tween 20 and then incubated at room temperature with the primary antibody TurboGFP (Evrogen Joint Stock, Russia), able to recognize both maxGFP fluorescence protein and its improved variant maxFP-Green. After incubation with horseradish peroxidase-conjugated secondary antibody (Bio-Rad Laboratories), detection was carried out by enhanced chemiluminescence according to the manufacturer's protocol (Amersham-Pharmacia Biotech. Italia). Densitometric analysis was performed by using a software program (Multi-Analyst, version 1.1, Bio-Rad Laboratories). All results were standardised using the signal obtained with β-actin antibody (Sigma).

*2.14. Statistical analysis*

Statistical significance of data were checked by analysis of variance and paired Student's *t* test. The corresponding probability (*P*) value <.05 or <.01 was considered to be significant.

## 3. Results

### *3.1. HNE effect on cell proliferation, differentiation and apoptosis in Caco-2 cells*

Repeated treatments with 1 μM HNE caused the inhibition of Caco-2 cell proliferation from Day 2 (Fig. 1A), until the end of the experiment (Day 4), as previously reported [44]. To determine

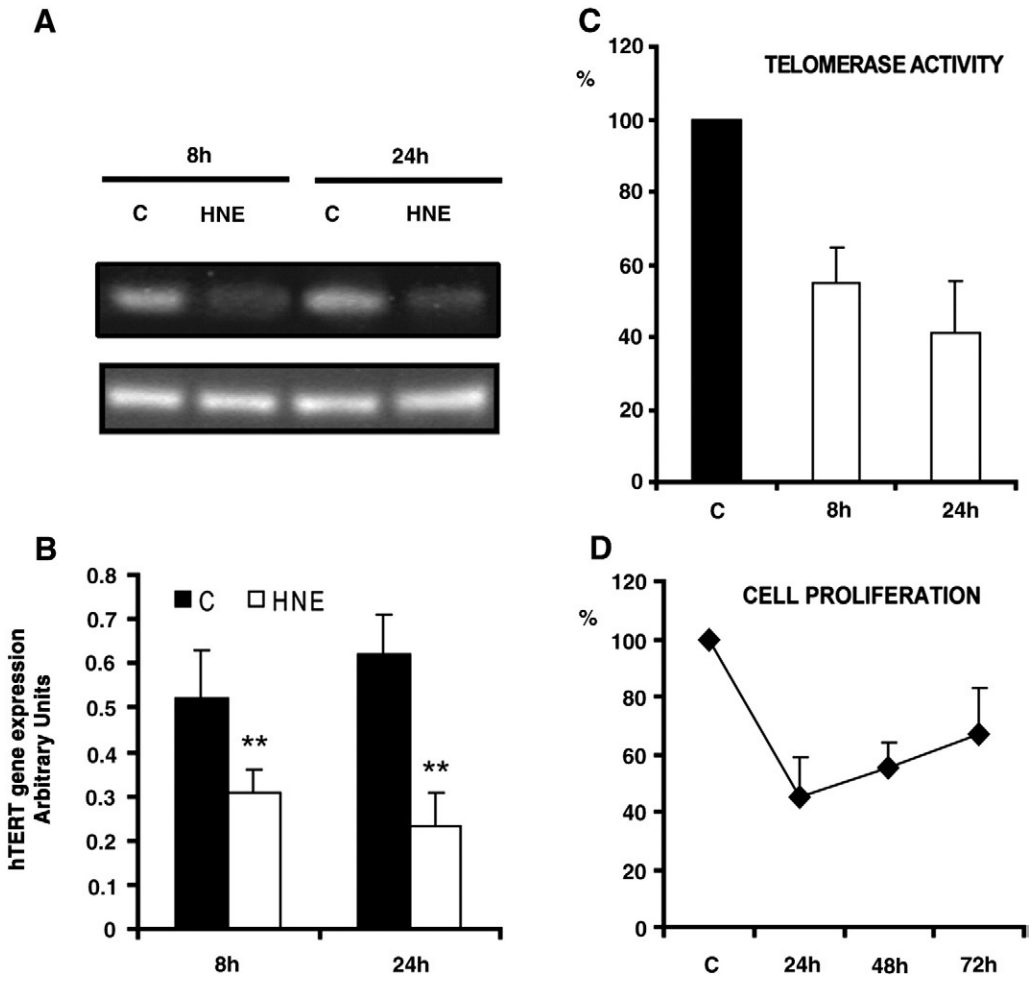


Fig. 3. *hTERT* expression, telomerase activity and cell proliferation in HNE-treated HT-29 cells. (A) *hTERT* mRNA levels determined by RT-PCR in Caco-2-untreated cells (C) and in HNE-treated cells (10 repeated treatments with 1 μM HNE) at the indicated time. (B) the relative quantification of RT-PCR products performed by densitometric scanning is shown. Data were normalized using the GAPDH signal and expressed as arbitrary densitometric units. Values represent the means±S.D. of three independent experiments. Variance analysis: *$P$<.05; **$P$<.01 vs. control. (C) Telomerase activity. The activity was evaluated at the indicated times in HT-29 untreated cells (C) and in HNE-treated cells (10 repeated treatments with 1 μM HNE) at the indicated time. Telomerase activity was calculated in terms of nanograms of DNA produced per microgram of protein from three independent experiments and reported in figures as percentage of control sample. (D) HT-29 cell proliferation in untreated (C) and HNE -treated cells (10 repeated treatments with 1 μM HNE). Cell proliferation was assessed by MTT assay, from four independent experiments and reported in figures as percentage of control sample.

whether the inhibition of growth was due to apoptosis, cells exposed to HNE were analysed by TUNEL test (Fig. 1, panel B). In these experiments, 10 mM butyrate, able to induce apoptosis in 23.0% of the cells, was used as positive control. A significant percentage of apoptotic cells was observed in HNE-treated cells, starting from 8.7% at 24 h and reaching 15.2% at 72 h.

HNE-induced differentiation in Caco-2 cells was also assayed by monitoring the number of domes, at different times after the treatments (Fig. 1C). Butyrate 2 mM, used as positive control, was able to induce more than 35 domes/cm$^2$ from Day 1. HNE, on the contrary, was not able to induce differentiation in Caco-2 cells.

### 3.2. HNE effect on hTERT expression and telomerase activity in Caco-2 cells

Fig. 2 shows the analysis of *hTERT* expression and telomerase activity in control Caco-2 cells and after HNE treatments. This aldehyde was able to down-regulate *hTERT* mRNA expression at 24 h from the beginning of treatments. After 48 h from the treatment, *hTERT* was still down-regulated, but its expression was higher than that detected at 24h (Fig. 2A-B). Telomerase activity (Fig. 2C) was also down regulated in HNE treated cells, paralleling *hTERT* expression.

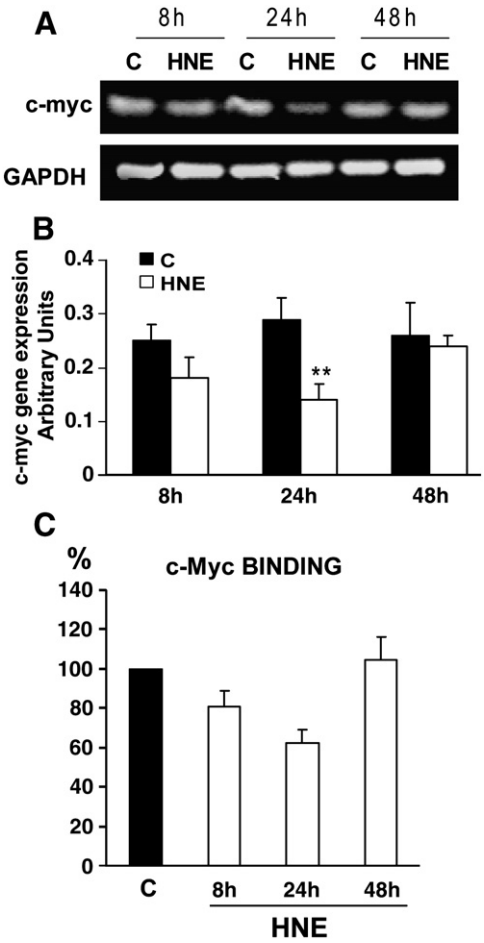


Fig. 4. Gene expression and DNA binding activity of c-*myc* in HNE-treated Caco-2 cells. (A) c-*myc* mRNA levels determined by RT-PCR in Caco-2-untreated cells (C) and in HNE-treated cells (10 repeated treatments with 1 μM HNE) at the indicated time. (B) the relative quantification of RT-PCR products performed by densitometric scanning is shown. Data were normalized using the GAPDH signal and expressed as arbitrary densitometric units. Values represent the means±S.D. of three independent experiments. Variance analysis: **$P$≤.01 vs. control. (C) DNA binding activity of c-Myc transcription factor in Caco-2 cells. Nuclear extracts were obtained from control (C) and HNE-treated cells (10 repeated treatments with 1 μM HNE) at the indicated time. DNA binding activity was quantified using an ELISA-based kit, as reported in Materials and methods. Results are expressed as a percentage with respect to the control cells and they are indicated as means±S.D. of three independent experiments.

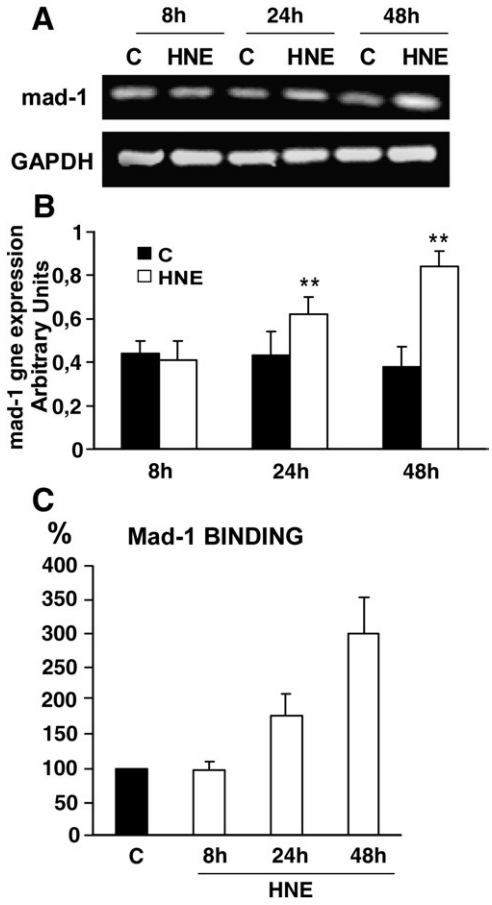


Fig. 5. Gene expression and DNA binding activity of mad-1 in HNE-treated Caco-2 cells. (A) mad-1 mRNA levels determined by RT-PCR in Caco-2-untreated cells (C) and in HNE-treated cells (10 repeated treatments with 1 μM HNE) at the indicated time. (B) the relative quantification of RT-PCR products performed by densitometric scanning is shown. Data were normalized using the GAPDH signal and expressed as arbitrary densitometric units. Values represent the means±S.D. of three independent experiments. Variance analysis: **$P$≤.01 vs. control. (C) DNA binding activity of Mad-1 transcription factor in Caco-2 cells. Nuclear extracts were obtained from control (C) and HNE-treated cells (10 repeated treatments with 1 μM HNE) at the indicated time. DNA binding activity was quantified using an ELISA-based kit, as reported in Materials and methods. Results are expressed as a percentage with respect to the control cells and they are indicated as means±S.D. of three independent experiments.

### 3.3. GSH content in HNE-treated Caco-2 cells

In Caco-2 control cells GSH content was 21.5±3.75 nanomoles of GSH per milligram of protein. Exposure to 1 μM HNE caused significant decreases in GSH content at 8 h (by 36% of inhibition with respect to the control), and at 24 h, GSH content returned to the control values (Fig. 2D).

### 3.4. HNE effect on hTERT expression, telomerase activity and cell proliferation in HT-29

In order to determine whether the effect of HNE on telomerase was a specific phenomenon on Caco-2 cells or a more common effect on colon cancer cells, telomerase activity and *hTERT*

expression, after HNE treatment, was also determined in human colon cancer HT-29 cells.

Fig. 3 shows the analysis of *hTERT* expression (Panels A–B) and telomerase activity (Panel C) in control and in HNE-treated HT-29 cells. HNE was able to down-regulate *hTERT* mRNA expression and telomerase activity at 8 and 24 h from the beginning of treatments. As observed in Caco-2 cells, HNE significantly reduced proliferation of HT-29 cells starting at 24 h (Fig. 3D).

### 3.5. HNE effect on expression and DNA binding activity of transcription factors involved in hTERT promoter regulation

The expression of c-*myc*, mad-1 and sp-1, the major transcription factors involved in the control of *hTERT* gene expression, was examined.

HNE was able to down-regulate c-*myc* mRNA expression in Caco-2 cells at 24 h (Fig. 4A–B) and Myc DNA binding activity paralleled c-*myc* expression (Fig. 4C).

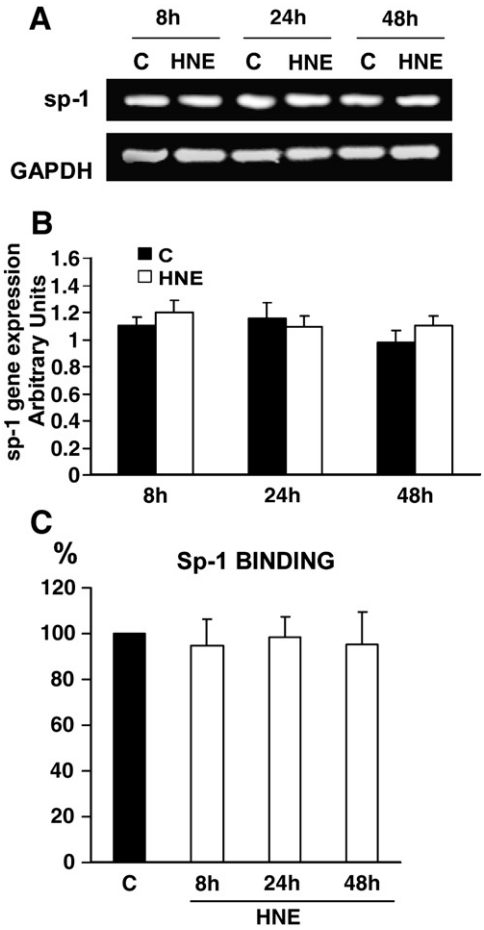


Fig. 6. Gene expression and DNA binding activity of sp-1 in HNE-treated Caco-2 cells. (A) sp-1 mRNA levels determined by RT-PCR in Caco-2-untreated cells (C) and in HNE-treated cells (10 repeated treatments with 1 μM HNE) at the indicated time. (B) the relative quantification of RT-PCR products performed by densitometric scanning is shown. Data were normalized using the GAPDH signal and expressed as arbitrary densitometric units. Values represent the means±S.D. of three independent experiments. Variance analysis: $^{**}P \leq .01$ vs. control. (C) DNA binding activity of Sp-1 transcription factor in Caco-2 cells. Nuclear extracts were obtained from control (C) and HNE-treated cells (10 repeated treatments with 1 μM HNE) at the indicated time. DNA binding activity was quantified using an ELISA-based kit, as reported in Materials and methods. Results are expressed as a percentage with respect to the control cells and they are indicated as means±S.D. of three independent experiments.

An up-regulation of mad-1 mRNA expression was observed at 24 and 48 h after HNE treatments (Fig. 5A–B). Accordingly, an increase of Mad-1 DNA binding activity (Fig. 5C) occurred at 24 and 48 h in HNE-treated cells.

The expression of sp-1 transcription factor or its DNA binding activity did not change after HNE treatment (Fig. 6A–C).

### 3.6. Effects of HNE in controlling hTERT promoter activity

To confirm the DNA binding assay results, we performed transient transfection of Caco-2 cells with plasmid constructs containing the proximal promoter region of the *hTERT* promoter (Ebox-*hTERT*-GFP) and its E-box deleted form (Ebox-less-*hTERT*-GFP), in control and HNE-treated cells, as described under Materials and methods. HNE treatment caused, at 24 h, a significant decrease (54.2%) in the activity of *hTERT* promoter containing the E-box and five GC-boxes, when compared to untreated controls (Fig. 7A).

To assess the role of the Sp-1 transcription factor in HNE-mediated inhibition of *hTERT* promoter, the E-box-less-*hTERT*-GFP construct, lacking the c-*myc* recognition sequence but still containing the Sp-1 binding sites, was used (Fig. 7A). After transfection, we did not observe any significant modulation of promoter activity in HNE-treated cells, compared with control cells.

The basal activities of the two promoters are different. A reduction of 50.1% in the untreated cells transfected with the Ebox-less-*hTERT*-GFP, with respect to those transfected with the Ebox-*hTERT*-GFP construct has been demonstrated.

When cells were transfected with pmaxGFP plasmid, containing a strong promoter, we did not observe any significant modulation of promoter activity after HNE treatments, with respect to control cells. Therefore, transfection efficiency was not affected by the aldehyde treatment (Fig. 7B). As expected, after transfection with the empty vector pmaxFP-Green-PRL, no signal was observed.

## 4. Discussion

Inhibition of cell proliferation, obtained with micromolar doses of HNE, has also been described in diverse tumour cell lines, such as in myeloid leukemia [8–10,21], neuroblastoma [16] and osteosarcoma [45] cells, underlying the importance of this aldehyde in controlling this parameter. In Caco-2 cells, HNE strongly inhibits proliferation, induces apoptosis in a small number of cells (15.2% at 72 h) and does not induce differentiation of this cell line. Thus, the antiproliferative effect exerted by the aldehyde was not related to differentiation induction nor to apoptosis, which only partially can contribute to the reduction of proliferation, but it may be related to the telomerase activity down-regulation. This phenomenon seems not only restricted to a specific type of colon cancer cell because we demonstrated that HNE is able to inhibit telomerase activity and *hTERT* expression also in another human colon carcinoma cell line, the HT-29 cells, suggesting that the effect of HNE on telomerase could be common to other colon cancer cells.

Although telomerase enzymatic activity can be regulated by different mechanisms, including alternative splicing, chaperon-mediated folding, phosphorylation and nuclear translocation [46–48], transcriptional control of the *hTERT* gene seems to be the major control mechanism [49]. Telomerase down-regulation by HNE in Caco-2 cells does *not* seem to *constitute an exception, as demonstrated by the inhibition of hTERT gene expression.* One of the best characterized activators of *hTERT* transcription is the oncogene c-Myc, which is able to bind specific E-box sequences through heterodimer formation with Max proteins. Switching from Myc/Max binding to Mad/Max can function as a repressor of the *hTERT* promoter activity [27,50]. The down-regulation of c-*myc* gene expression and the up-regulation of mad-1 expression, after HNE treatment, paralleled *hTERT* down-

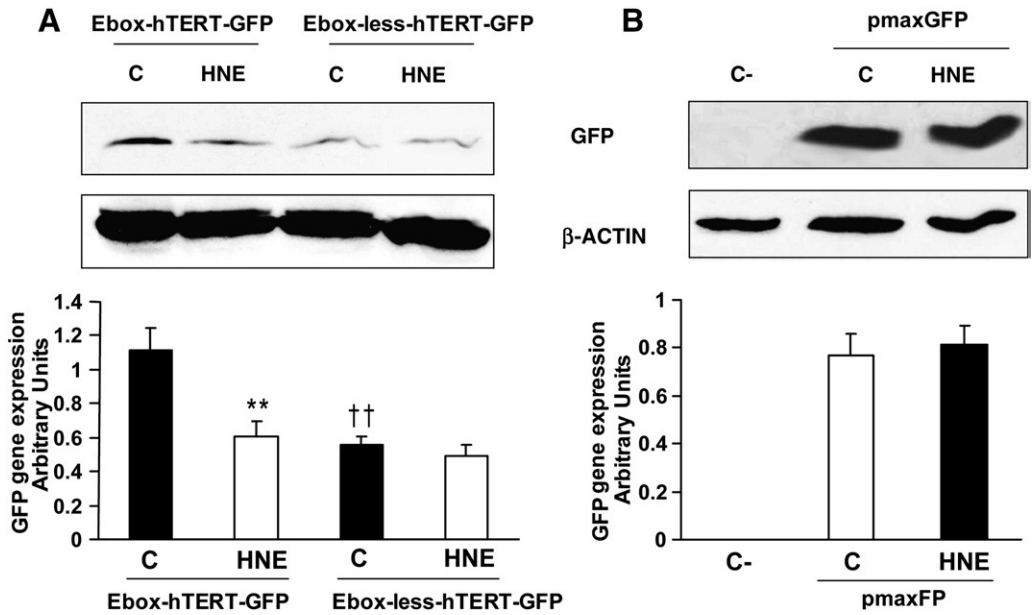


Fig. 7. Transient transfection with plasmid constructs containing the *hTERT* promoter in HNE-treated Caco-2 cells. (A) Promoter activity determined by Western blot analysis of GFP protein levels in cells transfected with two different constructs, Ebox-*hTERT*-GFP and Ebox-less-*hTERT*-GFP. Transfected cells were nontreated (C) or treated with HNE (10 repeated treatments with 1 μM HNE) and collected after 24 h from the beginning of the experiment. The graphic represents relative quantification of protein products performed by densitometric scanning. Data were normalized by using the β-actin signal and expressed as arbitrary densitometric units. Values represent the means±S.D. of three independent experiments. Variance analysis: $^{**}P<.01$ vs. respective control; $^{††}P<.01$ vs. Ebox-*hTERT*-GFP control. (B) Evaluation of the transfection efficacy by western blot analysis of GFP protein levels in cells transfected with the empty vector (C−) and with pmaxGFP plasmid containing the strong cytomegalovirus promoter pCMV. Cells were nontreated (C) or treated with HNE (10 repeated treatments with 1 μM HNE) and collected after 24 h from the beginning of the experiment. The graphic represents the relative quantification of protein products performed by densitometric scanning. Data are normalized by using the β-actin signal and expressed as arbitrary densitometric units. Values represent the means±S.D. of three independent experiments.

regulation. Moreover, the results of c-Myc and Mad-1 DNA binding assay are in agreement with the respective modulation of gene expression. Thus, the switch from c-Myc/Max to Mad/Max binding at the *hTERT* promoter may occur in HNE-treated Caco-2 cells.

Transient transfection experiments sustain the key role of E-box elements in the regulation of *hTERT* promoter activity, since, in Caco-2 cells, the basal activity of the E-box-*hTERT*-GFP is much higher than E-box-deleted *hTERT* promoter (Ebox-less-*hTERT*-GFP). Moreover, after HNE treatment, a strong reduction of *hTERT* promoter activity has been demonstrated in E-box-*hTERT*-GFP transfected cells, but not in Ebox-less-*hTERT*-GFP transfected cells.

Our results demonstrated that Sp-1 expression is not affected by HNE. Sp-1 can also be activated by post translational modification, such as phosphorylation, sumoylation and acetylation [51,52]. However, HNE treatment did not modulate Sp-1 DNA binding nor *hTERT* promoter activity in Ebox-less-*hTERT*-GFP transfected cells, suggesting that this transcription factor is not involved in our experimental model.

In order to investigate the contribution of other pathways in the down-regulation of telomerase activity, we investigated the role of GSH in our experimental model. GSH is a natural scavenger of HNE and Borras et al. [35] demonstrated that intracellular GSH content paralleled telomerase activity in 3T3 fibroblast. However, our results demonstrate that GSH can only partially contribute to the down-regulation of telomerase activity. Indeed, when Caco-2 cells were treated with HNE, we observed a depletion of GSH only at 8 h, when telomerase activity is not yet significantly inhibited. Thereafter GSH levels returned to control values while telomerase activity remained strongly inhibited. Considering all the results presented in this article, the major mechanism by which this aldehyde exerts the inhibition of telomerase activity seems to be the regulation of transcriptional control of the *hTERT* gene, by modulating the expression of transcription factors belonging to the Myc/Mad/Max network.

In recent years, a wide variety of noncanonical effects of telomerase, still important in carcinogenesis and independent of telomere lengthening, has been discovered [53]. In particular, telomerase has been shown to be able to inhibit apoptosis [54] and to affect cell cycle gene expression, such as the induction of p53, p21 [55] and the inhibition of cyclin D1 [56]. Intriguingly, we can hypothesize that the telomerase inhibition participates in the p21 up-regulation after HNE treatment in Caco-2 cells, as previously reported [44].

Interestingly, in accordance with the antiproliferative effect of HNE, here described, it has been reported that the extent of the lipid peroxidation process, as well as the concentration of the aldehydic end-products, decreased with the increase of tumor malignancy in colon adenocarcinoma [57,58]. This impairment of membrane lipid peroxidation, associated with tumor progression in colon cancer, has been suggested to be a further mechanism of evading cell growth regulation through reduced availability of antiproliferative aldehydic end-products [32].

Since the presence of PUFAs in the diet exposes epithelial colon cells to HNE, our results suggest that this aldehyde could contribute to cell growth control, suggesting a protective effect on colon mucosa. This action is carried out through the inhibition of telomerase activity and *hTERT* expression. These features were also demonstrated in human leukemic cells [21], thus suggesting that the inhibition of telomerase activity could be a general mechanism involved in the antiproliferative effect exerted by this aldehyde.

## References

[1] Dupertuis YM, Meguid MM, Pichard C. Colon cancer therapy: new perspectives of nutritional manipulations using polyunsaturated fatty acids. Curr Opin Clin Nutr Metab Care 2007;10:427–32.

[2] Law M. Dietary fat and adult diseases and the implications for childhood nutrition: an epidemiologic approach. Am J Clin Nutr 2000;72:3–11.
[3] Barrera G, Pizzimenti S, Dianzani MU. Lipid peroxidation: control of cell proliferation, cell differentiation and cell death. Mol Aspects Med 2008;29:1–8.
[4] Eckl PM. Genotoxicity of HNE. Mol Aspects Med 2003;24:161–5.
[5] Hu W, Feng Z, Eveleigh J, Iyer G, Pan J, Amin S, et al. The major lipid peroxidation product, *trans*-4-hydroxy-2-nonenal, preferentially forms DNA adducts at codon 249 of human p53 gene, a unique mutational hotspot in hepatocellular carcinoma. Carcinogenesis 2002;23:1781–9.
[6] Leonarduzzi G, Robbesyn F, Poli G. Signaling kinases modulated by 4-hydroxynonenal. Free Radic Biol Med 2004;37:1694–702.
[7] Awasthi YC, Sharma R, Sharma A, Yadav S, Singhal SS, Chaudhary P, et al. Self-regulatory role of 4-hydroxynonenal in signaling for stress-induced programmed cell death. Free Radic Biol Med 2008;45:111–8.
[8] Barrera G, Di Mauro C, Muraca R, Ferrero D, Cavalli G, Fazio VM, et al. Induction of differentiation in human HL-60 cells by 4-hydroxynonenal, a product of lipid peroxidation. Exp Cell Res 1991;197:148–52.
[9] Fazio VM, Barrera G, Martinotti S, Farace MG, Giglioni B, Frati L, et al. 4-Hydroxynonenal, a product of cellular lipid peroxidation, which modulates c-*myc* and globin gene expression in K562 erythroleukemic cells. Cancer Res 1992;52: 4866–71.
[10] Rinaldi M, Barrera G, Spinsanti P, Pizzimenti S, Ciafrè SA, Parella P, et al. Growth inhibition and differentiation induction in murine erythroleukemia cells by 4-hydroxynonenal. Free Radic Res 2001;34:629–37.
[11] Barrera G, Muraca R, Pizzimenti S, Serra A, Rosso C, Saglio G, et al. Inhibition of c-*myc* expression induced by 4-hydroxynonenal, a product of lipid peroxidation, in the HL-60 human leukemic cell line. Biochem Biophys Res Commun 1994;203: 553–61.
[12] Barrera G, Pizzimenti S, Serra A, Ferretti C, Fazio VM, Saglio G, et al. 4-hydroxynonenal specifically inhibits c-*myc* but does not affect c-*fos* expressions in HL-60 cells. Biochem Biophys Res Commun 1996;227:589–93.
[13] Pizzimenti S, Barrera G, Dianzani MU, Brüsselbach S. Inhibition of D1, D2, and A-cyclin expression in HL-60 cells by the lipid peroxydation product 4-hydroxynonenal. Free Radic Biol Med 1999;26:1578–86.
[14] Barrera G, Pizzimenti S, Laurora S, Moroni E, Giglioni B, Dianzani M. U. 4-Hydroxynonenal affects pRb/E2F pathway in HL-60 human leukemic cells. Biochem Biophys Res Commun 2002;295:267–75.
[15] Pizzimenti S, Laurora S, Briatore F, Ferretti C, Dianzani MU, Barrera G. Synergistic effect of 4-hydroxynonenal and PPAR ligands in controlling human leukemic cell growth and differentiation. Free Radic Biol Med 2002;32:233–45.
[16] Laurora S, Tamagno E, Briatore F, Bardini P, Pizzimenti S, Toaldo C, et al. 4-Hydroxynonenal modulation of p53 family gene expression in the SK-N-BE neuroblastoma cell line. Free Radic Biol Med 2005;38:215–25.
[17] Matés JM, Segura JA, Alonso FJ, Márquez J. Intracellular redox status and oxidative stress: implications for cell proliferation, apoptosis, and carcinogenesis. Arch Toxicol 2008;82:273–99.
[18] Wang J, Yi J. Cancer cell killing via ROS: to increase or decrease, that is the question. Cancer Biol Ther 2008;7:1875–84.
[19] Chen ZH, Niki E. 4-hydroxynonenal (4-HNE) has been widely accepted as an inducer of oxidative stress. Is this the whole truth about it or can 4-HNE also exert protective effects. IUBMB Life 2006;58:372–3.
[20] Uchida K. 4-Hydroxy-2-nonenal: a product and mediator of oxidative stress. Prog Lipid Res 2003;42:318–43.
[21] Pizzimenti S, Briatore F, Laurora S, Toaldo C, Maggio M, De Grandi M, et al. 4-Hydroxynonenal inhibits telomerase activity and *hTERT* expression in human leukemic cell lines. Free Radic Biol Med 2006;40:1578–91.
[22] Hiyama K, Hirai Y, Kyoizumi S, Akiyama M, Hiyama E, Piatyszek MA, et al. Activation of telomerase in human lymphocytes and hematopoietic progenitor cells. J Immunol 1995;155:3711–5.
[23] Bodnar AG, Ouellette M, Frolkis M, Holt SE, Chiu CP, Morin GB, et al. Extension of Life-Span by Introduction of Telomerase into Normal Human Cells. Science 1998; 279:349–52.
[24] Kim NW, Piatyszek MA, Prowse KR, Harley CB, West MD, Ho PL, et al. Specific association of human telomerase activity with immortal cells and cancer. Science 1994;266:2011–5.
[25] Bestilny LJ, Brown CB, Miura Y, Robertson LD, Riabowol KT. Selective inhibition of telomerase activity during terminal differentiation of immortal cell lines. Cancer Res 1996;56:3796–802.
[26] Xu D, Gruber A, Peterson C, Pisa P. Suppression of telomerase activity in HL60 cells after treatment with differentiating agents. Leukemia 1996;10:1354–7.
[27] Xu D, Popov N, Hou M, Wang Q, Björkholm M, Gruber A, et al. Switch from Myc/Max to Mad1/Max binding and decrease in histone acetylation at the telomerase reverse transcriptase promoter during differentiation of HL60 cells. Proc Natl Acad Sci U S A 2001;98:3826–31.
[28] Shay JW, Bacchetti S. A survey of telomerase activity in human cancer. Eur J Cancer 1997;33:787–91.
[29] Gryfe R, Swallow C, Bapat B, Redston M, Gallinger S, Couture J. Molecular biology of colorectal cancer. Curr Probl Cancer 1997;21:233–300.
[30] Kanamaru T, Tanaka K, Kotani J, Ueno K, Yamamoto M, Idei Y, et al. Telomerase activity and *hTERT* mRNA in development and progression of adenoma to colorectal cancer. Int J Mol Med 2002;10:205–10.
[31] Boldrini L, Faviana P, Gisfredi S, Donati V, Zucconi Y, Ursino S, et al. Evaluation of telomerase in the development and progression of colon cancer. Int J Oncol 2002; 10:589–92.
[32] Biasi F, Mascia C, Poli G. TGFB1 expression in colonic mucosa: modulation by dietary lipids. Genes Nutr 2007;2:233–43.
[33] Pierre F, Tache S, Guéraud F, Rerole AL, Jourdan ML, Petit C. Apc mutation induces resistance of colonic cells to lipoperoxide-triggered apoptosis induced by faecal water from haem-fed rats. Carcinogenesis 2007;28(2):321–7.
[34] Esterbauer H, Schaur RJ, Zollner H. Chemistry and biochemistry of 4-hydroxynonenal, malonaldehyde and related aldehydes. Free Radic Biol Med 1991;11: 81–128.
[35] Borras C, Esteve JM, Vina JC, Sastre J, Vina J, Pallardo FV. Glutathione regulates telomerase activity in 3T3 fibroblasts. J Biol Chem 2004;279:34332–5.
[36] Kyo S, Takakura M, Taira T, Kanaya T, Itoh H, Yutsudo M, et al. Sp-1 cooperates with c-Myc to activate transcription of the human telomerase reverse transcriptase gene (*hTERT*). Nucleic Acids Res 2000;28:669–77.
[37] Cong YS, Wen J, Bacchetti S. The human telomerase catalytic subunit *hTERT*: organization of the gene and characterization of the promoter. Hum Mol Genet 1999;8:137–42.
[38] Chantret I, Barbat A, Dussaulx E, Brattain MG, Zweibaum A. Epithelial polarity, villin expression, and enterocytic differentiation of cultured human colon carcinoma cells: a survey of twenty cell lines. Cancer Res 1988;48: 1936–42.
[39] Gelmini S, Caldini A, Becherini L, Capaccioli S, Pazzagli M, Orlando C. Rapid, quantitative nonisotopic assay for telomerase activity in human tumors. Clin Chem 1998;44:2133–8.
[40] Owens L, Belcher RVA. colorimetric micro-method for the determination of glutathione. Biochem J 1965;94:75–9.
[41] Horikawa I, Cable PL, Afshari C, Barrett JC. Cloning and characterization of the promoter region of human telomerase reverse transcriptase gene. Cancer Res 1999;59:826–30.
[42] Kyo S, Takakura M, Fujiwara T, Inoue M. Understanding and exploiting *hTERT* promoter regulation for diagnosis and treatment of human cancers. Cancer Sci 2008;99:1528–38.
[43] Shagin DA, Barsova EV, Yanushevich YG, Fradkov AF, Lukyanov KA, Labas YA, et al. GFP-like proteins as ubiquitous metazoan superfamily: evolution of functional features and structural complexity. Mol Biol Evol 2004;21:841–50.
[44] Cerbone A, Toaldo C, Laurora S, Briatore F, Pizzimenti S, Dianzani MU, et al. 4-Hydroxynonenal and PPARgamma ligands affect proliferation, differentiation, and apoptosis in colon cancer cells. Free Radic Biol Med 2007;42: 1661–70.
[45] Calonghi N, Boga C, Cappadone C, Pagnotta E, Bertucci C, Fiori J, et al. Cytotoxic and cytostatic effects induces by 4-hydroxynonenal in human osteosarcoma cells. Biochem Biophys Res Commun 2002;292:1502–7.
[46] Ulaner GA, Hu JF, Vu TH, Giudice LC, Hoffman AR. Tissue-specific alternate splicing of human telomerase reverse transcriptase (*hTERT*) influences telomere lengths during human development. Int J Cancer 2001;91:644–9.
[47] Liu K, Hodesn RJ, Weng N. Cutting edge: telomerase activation in human T lymphocytes does not require increase in telomerase reverse transcriptase (*hTERT*) protein but is associated with *hTERT* phosphorylation and nuclear translocation. J Immunol 2001;166:4826–30.
[48] Toogun OA, Dezwaan DC, Freeman BC. The hsp90 molecular chaperone modulates multiple telomerase activities. Mol Cell Biol 2008;28:457–67.
[49] Poole JC, Andrews LG, Tollefsbol TO. Activity, function, and gene regulation of the catalytic subunit of telomerase (*hTERT*). Gene 2001;269:1–12.
[50] Gunes C, Lichtsteiner S, Vasserot AP, Englert C. Expression of the *hTERT* gene is regulated at the level of transcriptional initiation and repressed by Mad1. Cancer Res 2000;60:2116–21.
[51] Bouwman P, Philipsen S. Regulation of the activity of Sp1-related transcription factors. Mol Cell Endocrinol 2002;195:27–38.
[52] Spengler ML, Guo LW, Brattain MG. Phosphorylation mediates Sp1 coupled activities of proteolytic processing, desumoylation and degradation. Cell Cycle 2008;7:623–30.
[53] Bollmann FM. The many faces of telomerase: emerging extratelomeric effects. Bioessays 2008;30:728–32.
[54] Rahman R, Latonen L, Wiman KG. *hTERT* antagonizes p53-induced apoptosis independently of telomerase activity. Oncogene 2005;24:1320–7.
[55] Lai SR, Cunningham AP, Huynh VQ, Andrews LG, Tollefsbol TO. Evidence of extra-telomeric effects of *hTERT* and its regulation involving a feedback loop. Exp Cell Res 2007;313:322–30.
[56] Jagadeesh S, Banerjee PP. Telomerase reverse transcriptase regulates the expression of a key cell cycle regulator, cyclin D1. Biochem Biophys Res Commun 2006;347:774–80.
[57] Biasi F, Tessitore L, Zanetti D, Cutrin JC, Zingaro B, Chiarpotto E, et al. Associated changes of lipid peroxidation and transforming growth factor beta1 levels in human colon cancer during tumour progression. Gut 2002;50: 361–7.
[58] Chiarpotto E, Scavazza A, Leonarduzzi G, Camandola S, Biasi F, Teggia PM, et al. Oxidative damage and transforming growth factor beta 1 expression in pretumoral and tumoral lesions of human intestine. Free Radic Biol Med 1997; 22:889–94.